Journal of Applied Polymer Science

Nanocomposite Piezoelectric Films of P(VDF-TrFE)/$LiNbO_3$

Van Son Nguyen,[1] Laurent Badie,[2] Emmanuel Lamouroux,[2] Brice Vincent,[1] Fabrice Domingues Dos Santos,[3] Maëlen Aufray,[4] Yves Fort,[2] Didier Rouxel[1]

[1]Institut Jean Lamour, Department P2M, UMR CNRS 7198, Faculté des Sciences et Techniques, Université de Lorraine, 54506, Vandœuvre-lès-Nancy, France

[2]Structure et Réactivité des Systèmes Moléculaires Complexes—UMR CNRS 7565, Faculté des Sciences et Techniques, Université de Lorraine, 54506, Vandœuvre-lès-Nancy, France

[3]Piezotech S.A.S, 9, rue de Colmar, 68220, Hésingue, France

[4]Centre Interuniversitaire de Recherche et d'Ingénierie des Matériaux, Institut National Polytechnique de Toulouse, 4 allée Emile Monso, BP 44362, 31030 Toulouse Cedex 4, France

Correspondence to: D. Rouxel (E-mail: didier.rouxel@univ-lorraine.fr)

ABSTRACT: Piezoelectric films were prepared by incorporation of lithium niobate ($LiNbO_3$) nanoparticles into copolymer of vinylidene difluoride and trifluoroethylene. Nanoparticles of $LiNbO_3$ with ferroelectric phase were successfully synthesized and dispersed homogenously by ultrasonication in the copolymer matrix without any surfactant or surface functionalization. The nanocomposites were fully characterized by electronic microscopy, X-ray diffraction, differential scanning calorimetry, dynamical mechanical analysis, and piezometer. Surprisingly, the copolymer matrix crystallinity and morphology were not affected by the incorporation of nanoparticles. Therefore the nanocomposites remained good mechanicals properties and high ferroelectricity coupled to nonlinear optical activity thanks to the noncentro symmetric space group of lithium niobate. This could be a novel approach to develop new multifunctional materials. © 2012 Wiley Periodicals, Inc. J. Appl. Polym. Sci. 129: 391–396, 2013

KEYWORDS: mechanical properties; nanoparticles; nanowires and nanocrystals; morphology; composites

Received 26 July 2012; accepted 19 October 2012; published online 16 November 2012
DOI: 10.1002/app.38746

INTRODUCTION

The development of new sensors, transducers, integrated optoelectronic, and piezoelectric devices requires the preparation of new materials that link mechanical, optical, and piezoelectric properties.[1,2] One possible way to reach this aim consists in the development of nanocomposite materials,[3,4] in which inorganic nanoparticles (NPs) embedded in a polymer matrix could allow the modulation of optical and piezoelectric properties with remaining mechanical properties.

On one hand, the vinylidene fluoride (VDF) based electroactive polymers are intensively used in research and industry in regard to their simplicity of use,[5–7] relatively low cost, versatility and easy forming. Poly(vinylidene fluoride-trifluoroethylene) (P(VDF-TrFE)) was chosen as a matrix since it exhibits remarkable ferroelectric (pyroelectric and piezoelectric) capabilities,[8] which could induce coupled effect between NPs and polymer matrix.

On the other hand, few nonpiezoelectric nanofillers like carbon nanotubes,[9] aluminum oxide[10] and piezoelectric ones such as barium titanate[11] and lead titanate[12] have been incorporated in this copolymer with different concentrations and configurations. Electrical properties of P(VDF-TrFE) nanocomposites were enhanced by adding nanofillers.[13–15] However, the crystallinity of P(VDF-TrFE) can strongly decreased at high concentration of gold and nickel nanowires[16] and its morphology also strongly modified with high loading of $CoFe_2O_4$ nanoparticles.[17] As optical and piezoelectric properties are concerned, lithium niobate ($LiNbO_3$) NPs appear to be one of the best candidates thanks to its bulk properties among noncentro symmetric space group.[18,19]

The aim of this work was to incorporate ferroelectric nanoparticles into ferroelectric polymer without disruption of morphology of the matrix and hence without degradation of its piezoelectric and mechanical properties. Therefore, the preparation and the characterization of nanocomposite films P(VDF-TrFE)/$LiNbO_3$ were reported, with special attention paid to the nanocomposite morphology and the crystallinity of the copolymer matrix, which mainly control the ferroelectric properties, the piezoelectric and mechanical properties of the obtained material.

Applied Polymer SCIENCE

The piezoelectric activity of nanocomposite filled with ferroelectric $LiNbO_3$ nanoparticles was compared with the results of non-ferroelectric Al_2O_3 nanoparticles in the previous study[10] for deeper understanding of the effect of ferroelectric nanoparticles at the macroscopic scale of nanocomposites.

EXPERIMENTAL

The synthesis procedure of $LiNbO_3$ was adopted from Aufray et al.[20] All experiments were conducted under argon atmosphere using classical Schlenk techniques. A Schlenk tube was loaded with 12.2 mmol of anhydrous niobium (V) chloride (ABCR, Strem chemicals) and 250 mL of freshly distilled toluene were added. When the temperature of the obtained solution reaches 110°C, six equivalents of LiH (Alfar Aesar) were added in one portion. The suspension was maintained under reflux during 20 h and then the solvent was removed under reduced pressure, leading to a dark gray powder. After an oxidation step of 20 h under air, the excess of LiH (1 eq.) was neutralized by the addition of ethanol. Then, the powder was rinsed with EtOH and centrifuged three times, to remove LiCl salt, which is the main byproduct of this preparation method. Finally, the powder was annealed at 550°C during 1 h under air atmosphere.

The copolymer of vinylidene difluoride and trifluoroethylene (P(VDF-TrFE)) (70/30 mol %), M_w = 1,370,000, PDI = 2.7 from Piezotech S.A.S. (France) was dissolved in methyl ethyl ketone (MEK) (Acros Organics) by stirring at 80°C to obtain a 14 wt % solution. To the copolymer solution, $LiNbO_3$ NPs were added at different weight ratios and then ultrasonicated to get homogeneous solutions. After that, the solutions were filtered at 2.7 μm to remove large dusts that may cause breakdown during polarization. In spite of the retention of the large clusters of nanoparticles during filtration, the resulting films were termed as 1, 3, 5, and 10% according to the weight ratios of $LiNbO_3$ added. The concentrations are kept relatively low to remain the conformability of the matrix and its processing facilities, which are the main advantages of organic materials. The solutions were casted onto a clean glass plate and dried in air at room temperature to get free-standing films of 20 × 20 cm^2 with thickness around 30 ± 2 μm, except specific indication. The spin coated films were made at 1000 rpm for 30 s and dry at 75°C on a hot plate to remove residual solvent. All of films were annealed at about 140°C in oven.

X-ray diffraction (XRD) was conducted using Cu Kα wavelength 1.54 Å (X'Pert Pro, PANAlytical) and the spectrum was compared to the JCPDS reference file for the NPs (number 85-2456). Environmental scanning electron microscopy (ESEM) (Quanta 600F, FEI Company) was used to observe the morphology of the cross section prepared by cryofracturing 3-μm spin-coated samples frozen in liquid nitrogen. Transmission electron microscopy (Philips CM 200) images were taken on films prepared by spin-coating directly on copper grid with a well dilute solution (1.4 wt %) to obtain a suitable thickness (around 100 nm) for this observation. Dynamic light scattering (DLS) (ZetaSizer NanoZS, Malvern Instruments) were carried out after the nanoparticles synthesis to measure cluster size in organic solution.

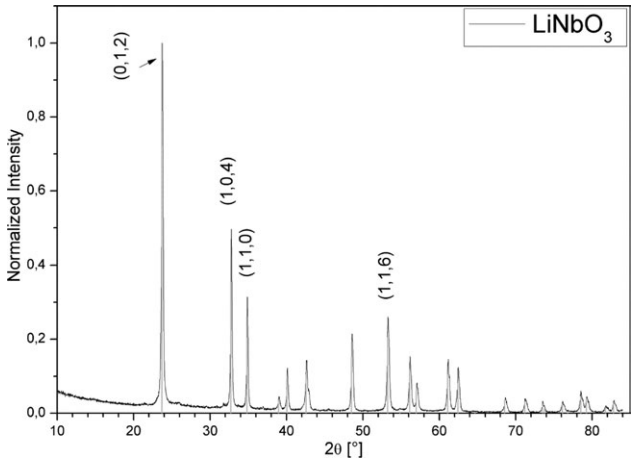

Figure 1. X-ray diffraction pattern of $LiNbO_3$ nanoparticles.

Differential scanning calorimetry (DSC 204, NETZSCH) was used to study the thermal properties of the nanocomposites. The films sealed in aluminum pans were heated from −70°C to 180°C with the heating rate set at 10°C min^{-1} in nitrogen atmosphere. The polymer crystallinity (X_c) was determined by equation[21]:

$$X_c = \frac{\Delta H_m + \Delta H_c}{\Delta H_0} \times 100$$

where ΔH_m and ΔH_c are the enthalpy of melting and Curie transition, respectively. The enthalpy of fusion of 100% crystalline (ΔH_0) of P(VDF-TrFE) 70/30 is 91.05 kJ g^{-1}.[21]

Dynamic mechanical analysis (DMA 242 C, NETZSCH) were conducted on around 350-μm thick films in tension mode and averaged over four samples. Measurements were performed between −100°C and 40°C at a rate of 2°C min^{-1}, at 10-Hz frequency.

To study piezoelectric properties, surfaces of 3 × 3 mm^2 of films were polarized in high electric field (>100 MV m^{-1}) using "dynamic-contact" method.[22,23] After polarization, the piezoelectric coefficient d_{33} was measured at 100 Hz using a Berlincourt-type Piezometer (Channel Products, Chesterland, OH).

RESULTS AND DISCUSSION

Structure

Structure and phase purity of the samples were investigated by XRD. For the $LiNbO_3$ nanoparticles (Figure 1), the four main peaks are attributed to the pure ferroelectric structure from the non-centrosymmetric phase R3c. It is worth to notice that this crystallographic structure leads to piezoelectric[24] and nonlinear optical (NLO) properties. Moreover, neither other phases nor rest from the starting materials were observed.

The properties of P(VDF-TrFE) are controlled by its crystalline ferroelectric phase.[5] Therefore, any change in crystallinity of the matrix induced by nanoparticles would lead to modification in ferroelectric properties of the matrix and hence of the nanocomposites. The ferroelectric phase (β-phase) of P(VDF-TrFE) crystals was characterized by the (110) and (200) reflections at 2θ = 19.7° in XRD patterns (Figure 2).[11,25] These peaks were not modified by the presence of $LiNbO_3$ nanoparticles.

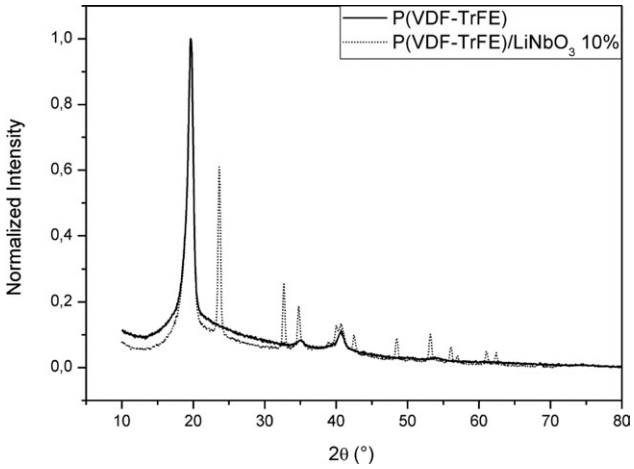

Figure 2. X-ray diffraction patterns of P(VDF-TrFE) and P(VDF-TrFE)/$LiNbO_3$ 10 wt %.

The result reveals that the nanoparticle did not affect the piezoelectric phase of the matrix copolymer in term of purity and percentage (confirmed by the DSC measurement, see part of thermal behavior).

Morphology

TEM micrograph (Figure 3) shows that $LiNbO_3$ primary particles exhibit pseudo-spherical morphology with a size ranging from 10 to 20 nm. Moreover, once dispersed in ethanol following the procedure adopted by Nguyen et al.,[25] DLS measurements show the presence of clusters with an average diameter (Z-average) of 360 nm with a high polydispersity index of 0.283 revealing that sintering process occurs during synthesis.

The microstructure of P(VDF-TrFE), which consisted of multiple stacks of lamellar, is shown by ESEM and TEM micrographs (Figures 4 and 5), such arrangement was also reported in literature.[10,26]

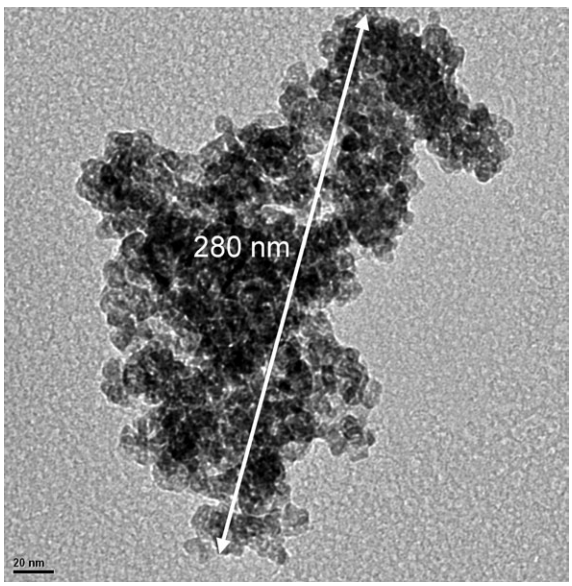

Figure 3. TEM micrograph of $LiNbO_3$ nanoparticle cluster.

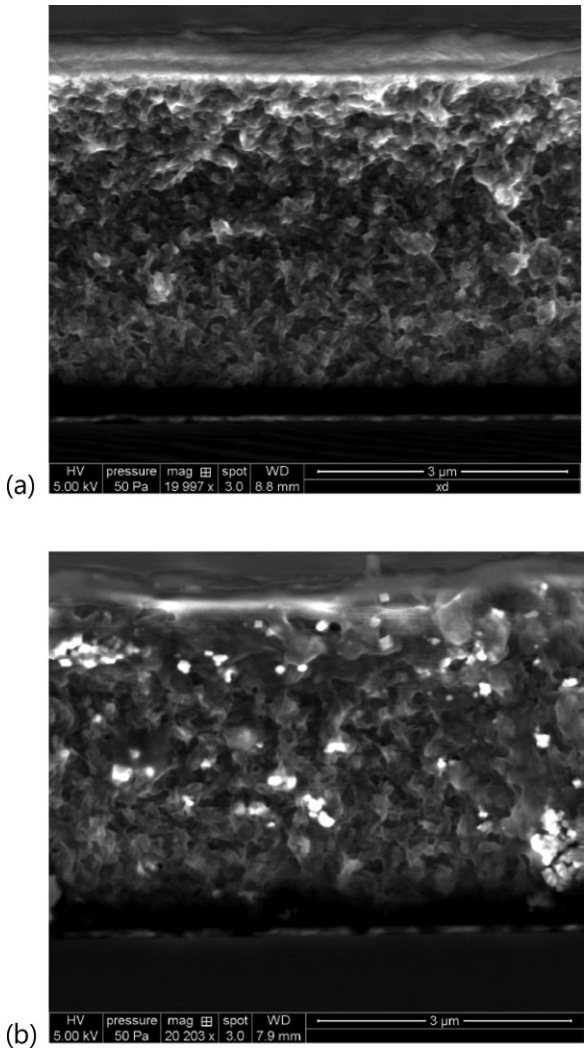

Figure 4. ESEM images of (a) P(VDF-TrFE) and (b) P(VDF-TrFE)/$LiNbO_3$ 10 wt %.

The nanoparticles did not have specific effect on the microdomain of P(VDF-TrFE) [Figure 4(b)], this morphology conservation will lead to keep all the matrix ferroelectric capabilities. Moreover, Figures 4(b) to 5(b) show that $LiNbO_3$ was homogeneously dispersed in the matrix with clusters size about 350 nm (determined graphically). This result was confirmed by DLS measurement proving the similar efficiency of the dispersion in copolymer solution and in ethanol with good stabilization. The stability without surfactant of $LiNbO_3$ in P(VDF-TrFE) solutions might be attributed to interaction between the fluorine in the copolymers and the oxide nanoparticles, similar stabilization being also observed for Al_2O_3 [10] TEM observations allow to measure filler density of four clusters per μm^2. There was neither phase separation nor decohesion between the constituents. Thus the copolymer matrix was not significantly modified by the introduction of nanoparticles up to 10 wt %. At higher concentration, there could be a risk of agglomeration of nanoparticles.[27] Furthermore, the dramatic decreases of crystallinity of the copolymer matrix were observed at high concentration of nanofillers.[16,28]

Applied Polymer SCIENCE

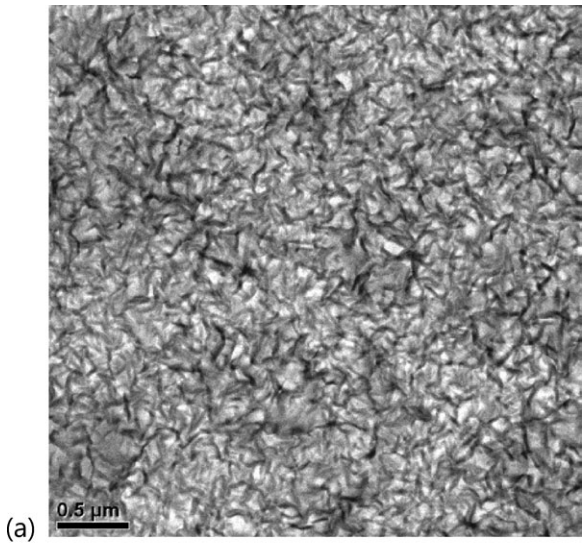

Figure 5. TEM micrographs of (a) P(VDF-TrFE) and (b) P(VDF-TrFE)/$LiNbO_3$ 10 wt %.

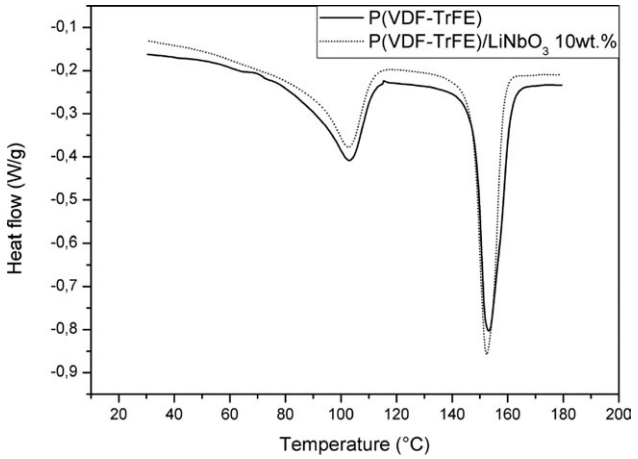

Figure 6. DSC heating curves of P(VDF-TrFE) and P(VDF-TrFE)/$LiNbO_3$ 10 wt %.

Thermal Behavior

The thermal behavior and crystallinity of the films have been studied by DSC (Figure 6). P(VDF-TrFE) film exhibited a melting peak around 153°C and a Curie peak (T_c), corresponding to the ferroelectric–paraelectric transition, around 103°C (Table I). The Curie and melting temperatures were almost unchanged by the insertion of $LiNbO_3$ in the copolymer. In addition, there was no difference in the percent crystallinity between the neat P(VDF-TrFE) and its nanocomposites. Contrary to phase transformation and inhibition effect of inorganic nanofillers on polymer crystal formation,[29–32] the phase and percent of crystallinity of the copolymer were conserved under given processing conditions. Nanoparticles often have a tendency to initiate the nucleation process for crystallization of polymer matrix. However, as can be seen from Figure 5(b), the size of $LiNbO_3$ particles was equivalent or even larger than the crystalline domain of P(VDF-TrFE), therefore it seems that the particle could not be located within the domain. The state of particle dispersion and effect of particles on polymer morphology depended on the relative size between particle diameter and polymer domain spacing.[27] Therefore the preservation of piezoelectric properties was also expected in addition to NLO from nanoparticles.

Mechanical Properties

In dynamic mechanical analysis, temperature dependence of storage modulus and damping factor (tan δ) are investigated. As shown in Figure 7, NPs addition improved moderately (5–10% for 10 wt % of fillers) the storage modulus over the entire temperature range. The effect of the filler addition is more obvious on the damping factor (Figure 8) with a viscous behavior enhancement of 30%. The tan δ curves show a broad peak around −32 and −36°C for the copolymer and its nanocomposite respectively, which corresponds to the glass transition temperature (T_g) of the matrix amorphous phase.[33]

As reported in the literature, nanofillers have usually a strong interaction with polymer matrix, which enhances the mechanical properties of the resulting nanocomposites.[10,30,32] In the present study, the nanoparticles did not have great effect on mechanical properties, for a concentration in nanoparticles ranging from 1 to 10 wt %. So, the results might be linked to a weak interaction between the inorganic filler and the copolymer matrix, as observed in other nanocomposites.[34] It is also recognized that the size of the inclusion plays an important role in this enhancement (the bigger are the filler, the lower is the reinforcement).[35] The T_g change indicates that there is less energy

Table I. DSC Parameters of P(VDF-TrFE)/$LiNbO_3$ with Various Contents of Nanoparticles

$LiNbO_3$ (wt %)	T_{Curie} (°C)	T_m (°C)	Crystallinity (%)
0	103	152	56
1	103	153	59
3	103	153	52
5	103	153	55
10	103	153	57

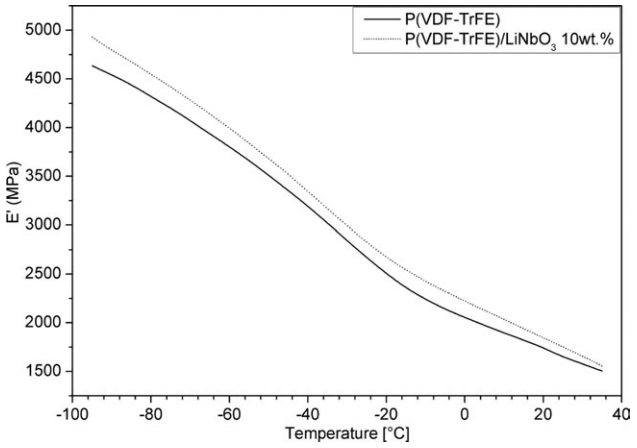

Figure 7. Temperature dependence of storage modulus for (a) P(VDF-TrFE) and (b) P(VDF-TrFE)/$LiNbO_3$ 10 wt %.

needed to have macromolecular movements between polymer chains in presence of nanoparticles, which certainly reveal local arrangements around them in the amorphous phase.

Piezoelectric Properties

To obtain high piezoelectricity for the nanocomposite material, the copolymer matrix had to be poled in strong electric field (>100 MV m^{-1}). The presence of agglomerates of particle and bad dispersion often led to electrical breakdown during such polarization. With quite good dispersion of nanoparticles in the polymer matrix, our nanocomposite films up to 10 wt % of nanofiller were successfully polarized. The piezoelectric coefficient d_{33} at room temperature of P(VDF-TrFE) and its nanocomposites are shown in Figure 9. The piezoelectric coefficient remained constant in the range of 20–22 pC N^{-1} upon nanoparticle addition thanks to the preservation of the crystallinity of the P(VDF-TrFE) matrix shown by the DSC experiment. Similar results were previously reported for P(VDF-TrFE)/Al_2O_3 nanocomposites.[10] It is worth noting that a disorganization of the copolymer matrix caused by nanoparticles will degrade the piezoelectric properties of the nanocomposites.

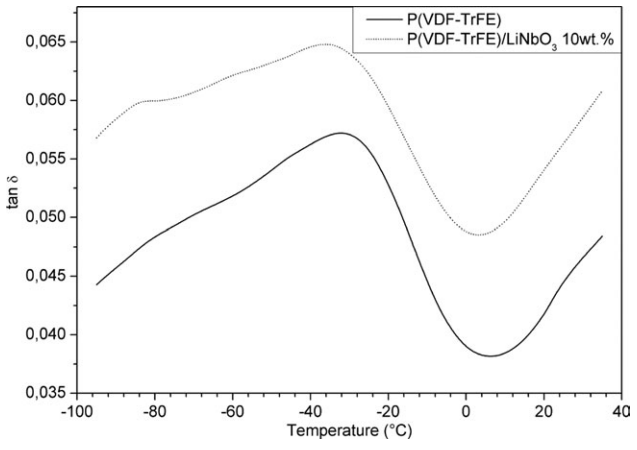

Figure 8. Temperature dependence of tan δ for (a) P(VDF-TrFE) and (b) P(VDF-TrFE)/$LiNbO_3$ 10 wt %.

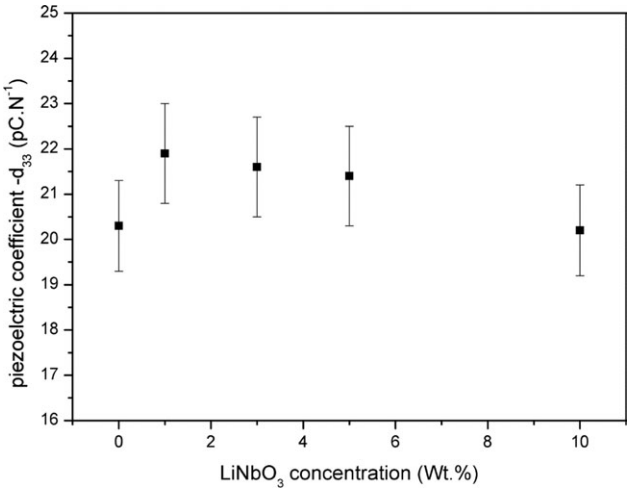

Figure 9. Piezoelectric coefficient of nanocomposite films as a function of $LiNbO_3$ concentration (error bars come from the accuracy of the setup).

In the previous study,[10] we showed that the incorporation up to 10 wt % of nonpiezoelectric Al_2O_3 nanoparticles does not alter the morphology and the crystallinity of the matrix and hence its properties. Thanks to the preservation of the matrix properties, the nanocomposites kept high piezoelectric constant with a clear gain in mechanical elasticity. Here, a similar preservation of the morphology and the crystallinity of the copolymer matrix was observed for nanocomposites of P(VDF-TrFE) filled with ferroelectric $LiNbO_3$ nanoparticles.

In this work, a specific orientation of ferroelectric nanoparticles by polarization at high temperature was not carried out. Therefore, we show that without this orientation, the piezoelectric activity of the LiNbO3 nanoparticles has no effect on the global piezoelectric properties of the nanocomposite. The piezoelectric activity of nanocomposite filled with ferroelectric nanoparticles without orientation depends only on the activity of the copolymer matrix and not on the nature of nanofillers. One should notice that to have optimal piezoelectric properties, the P(VDF-TrFE) matrix, $d_{33} = -20$ pC N^{-1}, and $LiNbO_3$ nanoparticles, $d_{33} = 6.3$ pC N^{-1}, must be polarized independently in opposite directions (charge constants with opposite sign).[36]

CONCLUSIONS

In summary, nanocomposite films based on P(VDF-TrFE) with embedded clusters of 10–20 nm $LiNbO_3$ nanoparticles were prepared by solution casting and spin-coating. The nanoparticle clusters ($\sim$ 360 nm) were homogenously dispersed in the copolymer matrix without surfactant, surface functionalization or specific treatment. The morphology and crystallinity of P(VDF-TrFE) were preserved in the presence of NPs, and the matrix mechanical properties were preserved with moderate enhancement. Moreover, nanocomposites still exhibited good piezoelectric activity without any polarization step for the nanoparticles. The result confirms that the ferroelectric nanoparticles without common orientation had only the same effect on the piezoelectric activity of nanocomposites as nonferroelectric ones. To expect a high contribution to composite

piezoelectric activity, nanoparticles have to be oriented by a specific polarization.

As the interesting properties of the P(VDF-TrFE) matrix are at least preserved by adding $LiNbO_3$ nanoparticles, it is feasible to fabricate multifunctional films for piezoelectric and/or pyroelectric properties by selecting the poling orientation of the matrix and nanoparticles. Moreover, $LiNbO_3$ exhibiting nonlinear optical properties, a good dispersion and orientation of nanoparticles in the matrix would confer those properties to polymer thin films for optoelectronic and acousto-optic applications. This could be a novel approach to develop new multifunctional materials for flexible devices, for instance in biological and acoustic wave applications.

ACKNOWLEDGMENTS

This work was funded by the French National Agency for Research (No. ANR-08-NANO-041) and labeled by the French competitiveness clusters PLASTIPOLIS and MATERALIA.

REFERENCES

1. Tabib-Azar, M. Microactuators: Electrical, Magnetic, Thermal, Optical, Mechanical, Chemical, and Smart Structures; Springer: Norwell, Massachusetts, **1998**.
2. Eldada, L. Telecom optical componentry: past, present, future. In: Fiber Optic Components, Subsystems, and Systems for Telecommunications; Tang, S.; Ren, X., Eds.; Spie-Int Soc Optical Engineering: Bellingham, **2001**. pp. 1–15.
3. Eschbach, J.; Rouxel, D.; Vincent, B.; Mugnier, Y.; Galez, C.; Le Dantec, R.; Bourson, P.; Krüger, J. K.; Elmazria, O.; Alnot, P. *Mater. Sci. Eng. C* **2007**, *27*, 1260.
4. Shi, Y.; Zhang, C.; Zhang, H.; Bechtel, J. H.; Dalton, L. R.; Robinson, B. H.; Steier, W. H. *Science* **2000**, *288*, 119.
5. Zhang, Q. M.; Bharti, V.; Kavarnos, G. In Encyclopedia of Smart Materials; Schwartz, M., Ed.; Wiley: New York, **2002**; p 807.
6. Mike Chung, T. C.; Petchsuk, A. In Encyclopedia of Physical Science and Technology; Robert, A. M., Ed.; Academic Press: New York, **2001**. pp. 659–674.
7. Nalwa, H. S. Ferroelectric Polymers: Chemistry, Physics, and Applications; M. Dekker: New York, **1995**.
8. Huang, C.; Klein, R.; Xia, F.; Li, H.; Zhang, Q. M.; Bauer, F.; Cheng, Z. Y. *IEEE Trans. Dielectr. Electrical Insulat.* **2004**, *11*, 299.
9. Qin, L.; Cheng, H.; Li, J. M.; Wang, Q. M. *Sens. Actuat. A: Phys.* **2007**, *136*, 111.
10. Hadji, R.; Nguyen, V.; Vincent, B.; Rouxel, D.; Bauer, F. *IEEE Trans. Ultrason. Ferroelectr. Frequency Control* **2012**, *59*, 163.
11. Fang, F.; Yang, W.; Zhang, M. Z.; Wang, Z. *Compos. Sci. Technol.* **2009**, *69*, 602.
12. Marra, S. P.; Ramesh, K. T.; Douglas, A. S. *Compos. Sci. Technol.* **1999**, *59*, 2163.
13. El Shafee, E.; El Gamal, M.; Isa, M. *J. Polym. Res.* **2012**, *19*, 1.
14. Song, Y.; Shen, Y.; Liu, H.; Lin, Y.; Li, M.; Nan, C.-W. *J. Mater. Chem.* **2012**, *22*, 8063.
15. Wang, J.; Wang, Y. E.; Li, S.; Xiao, J. *J. Polym. Sci. Part B: Polym. Phys.* **2010**, *48*, 490.
16. Lonjon, A.; Laffont, L.; Demont, P.; Dantras, E.; Lacabanne, C. *J. Phys. D Appl. Phys.* **2010**, *43*, 345401.
17. Zhang, J. X.; Dai, J. Y.; So, L. C.; Sun, C. L.; Lo, C. Y.; Or, S. W.; Chan, H. L. W. *J. Appl. Phys.* **2009**, *105*, 054102.
18. Weis, R. S.; Gaylord, T. K. *Appl. Phys. A: Mater. Sci. Process.* **1985**, *37*, 191.
19. Vincent, B.; Krüger, J. K.; Elmazria, O.; Bouvot, L.; Sanctuary, R.; Rouxel, D.; Alnot, P. *J. Phys. D: Appl. Phys.* **2005**, *38*, 2026.
20. Aufray, M.; Menuel, S.; Fort, Y.; Eschbach, J.; Rouxel, D.; Vincent, B. *J. Nanosci. Nanotechnol.* **2009**, *9*, 4780.
21. Clements, J.; Davies, G. R.; Ward, I. M. *Polymer* **1992**, *33*, 1623.
22. Bauer, F. *IEEE Trans. Ultrason. Ferroelectr. Frequency Control* **2000**, *47*, 1448.
23. Bauer, F.; Graham, R. A. *Ferroelectrics* **1995**, *171*, 95.
24. Mohanty, D.; Chaubey, G. S.; Yourdkhani, A.; Adireddy, S.; Caruntu, G.; Wiley, J. B. *Rsc Adv.* **2012**, *2*, 1913.
25. Nguyen, V. S.; Rouxel, D.; Hadji, R.; Vincent, B.; Fort, Y. *Ultrason. Sonochem.* **2011**, *18*, 382.
26. Koga, K.; Ohigashi, H. *J. Appl. Phys.* **1986**, *59*, 2142.
27. Lo, C.-T.; Chang, Y.-C.; Wu, S.-C.; Lee, C.-L. *Colloids Surf. A: Physicochem. Eng. Aspects* **2010**, *368*, 6.
28. Lonjon, A.; Demont, P.; Dantras, E.; Lacabanne, C. *J. Non-Cryst. Solids* **2012**, *358*, 236.
29. Bhatt, A. S.; Bhat, D. K.; Santosh, M. S. *J. Appl. Polym. Sci.* **2011**, *119*, 968.
30. Almasri, A.; Ounaies, Z.; Kim, Y. S.; Grunlan, J. *Macromol. Mater. Eng.* **2008**, *293*, 123.
31. Croce, F.; Appetecchi, G. B.; Persi, L.; Scrosati, B. *Nature* **1998**, *394*, 456.
32. Patro, T. U.; Mhalgi, M. V.; Khakhar, D. V.; Misra, A. *Polymer* **2008**, *49*, 3486.
33. Krüger, J. K.; Petzelt, J.; Legrand, J. F. *Colloid Polym. Sci.* **1986**, *264*, 791.
34. Vigolo, B.; Vincent, B.; Eschbach, J.; Bourson, P.; Marêché, J. F.; McRae, E.; Müller, A.; Soldatovy, A.; Hiver, J. M.; Dahoun, A.; Rouxel, D. *J. Phys. Chem. C* **2009**, *113*, 17648.
35. Yang, F.; Nelson, G. L. *J. Appl. Polym. Sci.* **2004**, *91*, 3844.
36. Ploss, B.; Ploss, B.; Shin, F. G.; Chan, H. L. W.; Choy, C. L. *Appl. Phys. Lett.* **2000**, *76*, 2776.